Stabilisation of soil organic matter with rock dust partially counteracted by plants

Wolfram Buss[a*]

Heath Hasemer[a]

Scott Ferguson[a]

Justin Borevitz[a]

[a] Research School of Biology, Australian National University, 134 Linnaeus Way, 2601 Canberra, Australia

*corresponding author: wolfram.buss@anu.edu.au

9 **Abstract**

10 Soil application of Ca- and Mg-rich silicates can capture and store atmospheric carbon

11 dioxide as inorganic carbon but could also have the potential to stabilise soil organic matter

12 (SOM). Synergies between these two processes have not been investigated. Here, we apply

13 finely ground silicate rock mining residues (basalt and granite blend) to a loamy sand in a pot

14 trial at a rate of 4% (equivalent to 50 t ha^{-1}) and investigate the effects of a wheat plant and

15 two watering regimes on soil carbon sequestration. Rock dust addition increased soil pH,

16 electric conductivity and soil-exchangeable Ca and Mg contents, as expected for weathering,

17 but decreased exchangeable levels of micronutrients Mn and Zn, likely related to soil pH.

18 Importantly, it increased mineral-associated organic matter by 22% due to the supply of

19 secondary minerals and associated sites for SOM sorption. Additionally, in the non-planted

20 treatments, rock supply of Ca and Mg increased soil microaggregation that subsequently

21 stabilised labile particulate organic matter as organic matter occluded in aggregates by 46%.

22 Plants, however, reduced soil exchangeable Mg and Ca contents and hence counteracted the

23 silicate rock effect on microaggregates and carbon within. We attribute this cation loss to

24 plant exudates released to solubilise micronutrients and hence neutralise plant deficiencies.

25 The effect of enhanced silicate rock weathering on SOM stabilisation could substantially

26 boost its carbon sequestration potential when pH and micronutrient effects are considered.

1 Introduction

27

28 Urgent action is required to avoid the most dangerous impacts of climate change. Such action

29 must include both significant reduction in greenhouse gas emissions, and atmospheric

30 greenhouse gas removal largely via land change (IPCC, 2022). Several promising greenhouse

31 gas removal methods are based on utilising natural cycles to capture and store atmospheric

32 carbon dioxide (Buss, Yeates, et al., 2021; Fuss et al., 2018). These include soil organic

33 carbon from plants and enhanced rock weathering.

34 During natural weathering of Ca- and Mg-rich silicates, bicarbonate (HCO_3^-) is formed,

35 capturing CO_2 from the atmosphere (largely as CO_2 respired from plants and soil

36 microorganisms) (Beerling et al., 2018; Hartmann et al., 2013). Follow-up reactions can

37 produce solid carbonates that sequester carbon for the long-term. The mafic rock basalt is one

38 of the most promising rock types for large-scale carbon capture and storage since it is

39 abundant, weathers rapidly and is low in heavy metal contaminants potentially harmful for

40 soil and plant growth. The weathering rates are highly dependent on rock particle size; 1 mm

41 sized spheres of even the most reactive Ca- and Mg-rich silicates take thousands of years to

42 dissolve (Hartmann et al., 2013). However, grinding rocks to a particle size of <100 µm can

43 result in weathering and carbon drawdown on a societal relevant scale (Holdren & Speyer,

44 1985; Renforth, 2012). Unfortunately, across multiple studies into the weathering rates of Ca-

45 and Mg-rich silicates in systems reflecting natural soil-plant conditions, CO_2 sequestration

46 rates were measured differently and varied by a factor of 1,000 (Amann et al., 2020; Haque et

47 al., 2019, 2020; Kelland et al., 2020; ten Berge et al., 2012). This demonstrates the need for

48 further studies that investigate enhanced weathering of globally available materials, such as

49 mining residues, using field soils and plants but grown in controlled conditions and measured

50 consistently across multiple interacting factors.

51   Soil organic carbon exists in natural systems as soil organic matter (SOM) and typically

52   enters the soil system as plant-derived particulate organic matter (POM), which is labile and

53   easily decomposed (Lavallee et al., 2020; Poeplau et al., 2018). Soil aggregates can

54   physically protect POM, which is called aggregated organic matter (AggOM), and minerals

55   can sorb partially decomposed POM fragments, so-called dissolved organic matter (DOM), to

56   its surfaces to form mineral-associated organic matter (MAOM) (Abramoff et al., 2018;

57   Hemingway et al., 2019; Poeplau et al., 2020). Both processes increase the retention and

58   stability of SOM in soil. Soil aggregates are formed through various soil processes that bind

59   together soil particles, such as activity from fungi hyphae and roots, or soil cementing agents,

60   including Ca, Mg, Al and Fe (Amezketa, 1999). The main components of soil responsible for

61   MAOM formation are clay and short-order Fe and Mn minerals formed from weathering of

62   primary minerals (Kleber et al., 2015; Singh et al., 2018). Polyvalent cations, such as Ca, Mg,

63   Al and Fe, also have a key function in facilitating sorption of DOM to mineral surfaces

64   through cation bridging; the connection of (predominantly) negatively charged clay surfaces

65   with negative functional groups of DOM (Kleber et al., 2015; Singh et al., 2018).

66   Synergies between enhanced rock weathering for both the formation of inorganic carbon for

67   direct carbon drawdown and the formation of secondary minerals and polyvalent cations for

68   stabilisation of SOM could significantly enhance its carbon sequestration potential and have

69   soil health co-benefits. Yet studies in this area that investigate the factors that influence its

70   potential are lacking.

71   Both rock weathering rates and SOM formation and decomposition reactions are affected by

72   soil water availability and plant activity. Higher precipitation and increased water flow

73   accelerates rock weathering (Brady et al., 1999; G. Li et al., 2016; White & Blum, 1995) and

74   water availability also governs microbial processes responsible for SOM decomposition and

75   affects plants that supply carbon into soil. Therefore, precipitation has a strong effect on

76   SOM levels (Luo et al., 2017) and the SOM content is typically higher in areas with more

77   precipitation (Alvarez, 2005; Wiesmeier et al., 2019). Plants can significantly increase rock

78   weathering rates by up 10-fold (Bormann et al., 1998; Cochran & Berner, 1996; Hinsinger et

79   al., 2001). Plants also provide the foundation for SOM formation through rhizodeposits from

80   living plants and litter from dead plants. Yet, they can also accelerate the decomposition of

81   existing SOM through various processes summarised under the term positive priming

82   (Keiluweit et al., 2015; Kuzyakov, 2010). The effects of plants and water could significantly

83   influence the potential synergies of rock weathering on SOM and inorganic carbon

84   sequestration.

85   In this study, to simulate potential field conditions, bulk mining residues (basalt, granite

86   blend) were applied to a sandy loam and field climatic conditions were replicated in a growth

87   chamber under controlled conditions. The effects of wheat plants and watering on rock

88   weathering, microbial composition and SOM content of different stability were investigated.

89   Further, the soil available and plant tissue elemental contents were analysed to understand the

90   mechanisms behind the soil response. The hypothesis was that weathering of Ca- and Mg-

91   rich silicates can increase both inorganic and organic carbon storage.

2 Materials and Methods

2.1 Soil and rock samples

The soil was agricultural topsoil (0-20 cm) sourced in 2020 from Young in central New South Wales, Australia. The soil was dried and stored for ~12 months before it was used in the incubation trial. It had a pH (in water) of 5.68 and was classified as loamy sand (USDA classification). The cation exchange capacity was 2.3 $cmol_+$ kg^{-1} and the total carbon and nitrogen contents were 0.88% and 0.045%, respectively. More details about the soil with full characterisation can be found in SI Table 1.

The rock mining residues were sourced from Victoria in Australia (Cohuna and Carisbrook) and comprise of both basalt and granite. The rock was ground with a pug mill and sieved to <90 µm with a p80 (80% of particles with a diameter less than specified size) of 50 µm. Data on X-ray diffraction and full acid digestion followed by inductively coupled plasma (ICP) – mass spectrometry (method ME-MS61 using perchloric, nitric, hydrofluoric and hydrochloric acids) and particle size using a Mastersizer 2000 (Malvern Panalytical; Malvern, UK) are shown in Table 1 and full particle size distribution of both materials in SI Figure 1.

2.2 X-ray diffraction of rock sample

Samples were pre-ground and sieved to <90 µm, then spiked with 20 wt% Al_2O_3 (Baikalox polishing corundum) and manually ground finely in an agate mortar in acetone. The suspension was pipetted on low-background holders (quartz), and dried. Powder X-ray diffraction analysis was carried out with a Malvern Panalytical Empyrean Series 3 diffractometer that was equipped with Bragg-Brentano[HD] divergent beam optic and a PIXcel[3D] detector (1D scanning mode, 3.347° active length), using CoKa radiation. Samples were analysed over a range of 4-85° 2q, with step width of 0.0131303° 2q and a total dwell time of 98 s/step, while spinning samples horizontally. Phase identification was carried out

116 with the software Diffrac*Plus* Eva 10 (2004; Bruker AXS GmbH, Karlsruhe, Germany) and

117 ICDD PDF-2 database (2004; PDF-2. International Centre for Diffraction Data, Newtown

118 Square, PA, USA), and quantification with Siroquant V4 (Taylor, 1991) and Highscore Plus

119 4.8 (2018; Malvern Panalytical B. V., Almelo, The Netherlands).

2.3 Soil incubation / wheat plant trial

121 The soil was sieved to <10 mm to remove large root and other plant structures. Soil or

122 crushed rock-soil mix (1.2 kg total) was filled into round pots 11 cm diameter and 11 cm high

123 with drain holes. Crushed rock was pre-mixed with the soil in ziplock bags at a rate of ~4%

124 w/w (equivalent to 50 t ha^{-1}). After watering, pre-germinated wheat seedlings (*Triticum*

125 *aestivum*, Condo variety) were planted into the centre of the pots (half of the pots were

126 planted).

127 A full-factorial design with treatments of rock/no rock, wheat/no wheat and low/high water

128 was used with 8 pot replicates (64 pots in total). No fertiliser was applied, and the pots were

129 kept in a growth chamber in a randomised block design for ~6 months simulating the diurnal

130 and seasonal light and temperature regime of central New South Wales, Australia, the origin

131 of the soil (temperature profile of ~8-10°C at night and ~18-25°C during the day). Pots were

132 watered with pre-determined amounts of tap water depending on high and low water

133 treatments. The high-water treatment received 100 mL of water three times a week and the

134 low water treatment 100 mL and 50 mL water each week. In some weeks lower/high

135 watering was necessary depending on plant growth stage resulting in 7 L and 4 L of water in

136 total for the high- and low-water treatments, which corresponds to ~740 and 420 mm

137 precipitation over the 6 months. This is approximately equivalent to the annual lower and

138 higher end of the precipitation in the area the soil and light/temperature regime were adapted

139 from.

140   At the end of the ~6 month-period, the plants and their roots were pulled out of the soil and

141   partitioned into roots, shoots and head (seeds/grain), dried at 105°C and weighed. Centrifuge

142   tubes (50 mL) were used to take soil samples from the area under the plant at harvest (3 cm

143   deep core). The soil samples were dried in the oven at 40°C for 3 days.

2.4 Soil analysis

2.4.1 Carbon analysis

146   A soil subsample (~400 mg) was ground, and the contents of carbon and nitrogen were

147   determined with a VarioMax 3000 (Elementar, Germany) (peak anticipated N: 210 s, oxygen

148   dosing time: 15 s, oxygen dosing: 70 ml min^{-1}, furnace temperatures: 900°C, 900°C and

149   830°C; helium as carrier gas). The inorganic carbon content was determined through prior

150   soil acidification using 1 M HCl until no gas release was visible.

2.4.2 Three-pool soil carbon fractionation

152   Full details about the soil carbon fractionation that distinguishes free POM, AggOM and

153   MAOM is described previously (Buss, Sharma, et al., 2021). In short: 10 g of soil was shaken

154   with a total volume of 50 mL of deionised water. Wet sieving was performed using 70 µm

155   sieves. For separating POM and AggOM sodium iodide adjusted to a density of 1.8 g cm^{-3}

156   was used. [33]The samples were centrifuged at 3000 rpm for 10 min and POM and AggOM

157   were separated by decanting the content of the tube onto a Whatman No. 2 filter paper. To

158   remove sodium iodide residues, the AggOM fraction was washed with deionised water. The

159   MAOM fraction (derived from the sieving step; <70 µm) was separated from the liquid

160   fraction via centrifugation at 3000 rpm for 30 min.

161   The carbon content within each fraction was analysed using a combustion method (details

162   above). The aqueous fraction was analysed for electric conductivity (EC) with a ProLab 5000

163   pH/EC meter (SI Analytics; Germany) and a suite of elements using ICP (details about ICP

164   below). The elemental content determined in this fraction is referred to as "water-extractable

165   content" in the following.

2.4.3 Two-pool soil carbon fractionation

167   The AggOM fraction comprises both occluded POM, protected from decomposition, but also

168   aggregated clay and silt particles that contain sorbed carbon (MAOM), sourced from either

169   plant exudates or residual POM decomposition (SI Figure 2). To further separate AggOM

170   into occluded (and free) POM and MAOM, so to investigate whether indeed carbon was

171   occluded in aggregates or whether it was only sorbed to the extra mineral surfaces provided

172   by the weathered rock, a second fractionation based on previous work (Cotrufo et al., 2019)

173   with some modifications was applied on a subset of samples (no rock-no plant; rock-no plant;

174   rock-plant).

175   A solution with 0.5% hexameta phosphate was prepared, and 30 mL added to 50 mL

176   centrifuge tubes that contained 2.5 g of soil and 2 glass beads. The tubes were shaken at 150

177   rpm for 18 hours and then sieved through 70 µm sieves (free and occluded POM). The

178   MAOM fraction was subsequently separated from the aqueous fraction through

179   centrifugation at 3000 rpm for 30 min. The free and occluded POM, MAOM and aqueous

180   fraction were all analysed for their carbon content.

2.4.4 ICP-Optical Emission Spectroscopy (ICP-OES)

182   The aqueous fractions recovered from the fractionation described under 2.3.2 were analysed

183   with an ICP-OES 5110 (Agilent; Santa Clara, CA, USA) for 20 elements. The ICP multi-

184   element standard solution Intelliquant No.1 and 2 from Agilent were used for calibration

185   using following concentrations: calibration blank, 0.01, 0.05, 0.1, 0.01, 1, 5, 10 and 50 mg L^{-1}

186   ^{1}. The 1 ppm standard was used as internal quality control.

2.4.5 Soil aggregation test

Soil aggregation was tested on a sub-set of samples (no rock-no plant; rock-no plant; rock-plant) to investigate which aggregates where increased in the rock-no plant treatment that resulted in the elevated AggOM contents. To determine soil aggregates, 7 sieves (sizes: 1000, 500, 400, 300, 200 and 70 µm; pluriStrainer, pluriSelect, Leipzig, Germany) were stacked on 50 mL centrifuge tubes. Suction was applied with a syringe to facilitate filtering of 1 g of soil and 500 mL of water through the sieves. Subsequently, the sieves were dried and weighed. The amount of soil in the <70 µm fraction was determined by the difference in mass.

2.4.6 Soil pH measurement

The soil pH was measured by shaking 1.5 g of soil with 30 mL of either deionised water or 0.01 M $CaCl_2$ in 50 mL tubes at 150 rpm for 1 hour. Tubes were left to settle for 20 min before the pH was measured with a ProLab 5000 pH/EC meter (SI Analytics; Germany).

2.5 Plant elemental content

Representative samples of grain, stem and roots (250 mg) were digested in 9 mL concentrated HNO_3 and 1 mL H_2O_2 in a microwave digester (Milestone ETHOS UP) at 210°C and 1800 W for 35 min. Samples were subsequently diluted to 2% HNO_3 and analysed via ICP-OES (as described above).

2.6 Microbial composition via shotgun metagenomics

Full details about the method to determine microbial composition was described previously (Buss, Sharma, et al., 2021). In short: a commercial DNA extraction kit (DNeasy PowerSoil Pro Kit, Qiagen, Hilden, Germany) was used for extracting DNA from the dried soil and the samples were barcoded with the "Native Barcoding kit" (Oxford Nanopore Technology, Oxford, UK) and run on a Flongle flow cell (Oxford Nanopore Technology, Oxford, UK). Data were basecalled and demultiplexed with Guppy (version: 5.0.7; Oxford Nanopore

211   Technology, Oxford, UK and all short (<200 bp) and low quality (<q7) sequences were

212   removed with NanoPack (De Coster et al., 2018).

213   Sequences were blasted against the NCBI nucleotide database version 5 (Sayers et al., 2021).

214   The taxonomic ID for the single best blast hit per sequence was extracted. Sequences without

215   a match and operational taxonomic units (phylum, class or order) that were only detected

216   once in a sample were excluded. Sequences matching an operational taxonomic unit (phylum,

217   class or order) observed in less than 8 samples (each treatment had 8 replicates) were also

218   filtered out.

219   2.7 Statistics

220   Statistical analyses were conducted in R (2022.12.0) and most visualisations in SigmaPlot

221   (Systat Software Inc; San Jose CA, USA). Analysis of variance and Tukey post-hoc tests

222   were conducted in R using the aov and TukeyHSD functions.

223   Microbial data were processed with Analysis of compositions of microbiomes with bias

224   correction (ANCOM-BC) on phyla, class and order level using the ANCOMBC2 package in

225   R (H. Lin & Peddada, 2020). The method normalises the data and checks for statistical

226   differences based on treatment effects. In addition, the row microbial count data (on phylum,

227   class and order level) were used for clustering using Non-Metric Multi-Dimensional Scaling

228   (NMDS) (vegan package; metaMDS; Bray-Curtis dissimilarity matrix) and NMDS 1 and 2

229   were subsequently plotted. PERMANOVA (vegan package in R) was used to check for

230   significant differences as a result of rock, plant and water treatments.

3 Results

3.1 Rock weathering, soil minerals and plant uptake

The inorganic carbon was not different between the control and rock amended treatments (Figure 1A). However, rock dust addition increased soil pH and EC immediately after application to soil (blue - rock dust baseline in Figure 1B and C) and the rock effect persisted throughout the incubation (significant rock effect on pH and EC). EC decreased from the baseline values in both the soil only and rock amended treatments. Plants and a high-water treatment accelerated EC decrease (Figure 1C).

Water-extractable Ca and Mg contents in soil increased significantly after rock addition as expected for weathering, but the plant effect eliminated this and decreased water-extractable Ca and Mg down to values comparable to the no-rock control treatments (Figure 1D, E). Rock addition also increased the ammonium acetate-extractable (exchangeable) Ca and Mg contents, and the levels were significantly higher after the incubation for both planted and unplanted treatments (Figure 1G and H). There was an initial peak of Ca and Mg release of fresh rock-sand samples, but we could not detect associated changes with any bi-(carbonate) levels in water-extractions (data not shown), predicted as part of alkalinity release during rock weathering. In contrast to the water-extractable contents of Ca and Mg that decreased over the course of the incubation compared to the baseline value (blue line in Figure 1D, E), the ammonium acetate-exchangeable content increased (Figure 1G, H). The increase in soil exchangeable Ca is highly significant in all rock treatments (p-values < 0.0001). For Mg only the two unplanted treatments were significantly higher than the rock-sand baseline (low water: $p = 0.00003$; high water: $p = 0.00029$). The water-extractable Si content did not change as a result of rock addition (Figure 1F), but the exchangeable content increased by 3-4-fold (Figure 1I).

255   There was no overall effect of rock addition on plant biomass or the individual plant parts (SI

256   Figure 3) and no effect on uptake (total mass) of Ca and Mg into plant tissue (SI Figure 4).

257   But the plant grain Ca content (mg Ca per kg plant biomass) and total Ca uptake into grain

258   (mg Ca per plant) significantly increased because of rock addition ($p = 3.9 \ 10^{-6}$; SI Figure 4

259   and SI Figure 5). Plant tissue contents (stem and root) and total uptake of Si in plant tissue

260   increased significantly due to rock application (SI Figure 4 and SI Figure 5).

261   Rock amendment significantly decreased soil exchangeable contents, plant tissue levels and

262   plant uptake of micronutrients Mn and Zn (Figure 2). The rock treatment did not significantly

263   reduce exchangeable Fe levels (Figure 2A3), yet within the rock treatments, plant addition

264   decreased exchangeable Fe (Figure 2A3) and Zn (Figure 2A2). Rock significantly decreased

265   the content and total uptake of Fe into grains (Figure 2C3).

266 3.2 Soil carbon content and three-pool soil carbon fractionation

267   The total soil carbon content decreased over the course of the incubation in all treatments

268   (red/blue lines in Figure 3A). The rock-amended soils started with a slightly lower soil

269   carbon content (blue line) than the control (red line) because the mass of rock addition diluted

270   the soil carbon content (rock 0.075% C; soil 0.88% C).

271   By the end of the experiment, rock addition led to a 16% higher total carbon content across

272   all treatments (rock effect: $p = 0.00007$; Figure 3A) and an even 32% higher content when

273   only the non-planted treatments are considered. Plants partially counteracted the rock effect

274   decreasing soil carbon content (rock:plant effect: $p = 0.00006$). Overall, the three treatments

275   and their interactions explained 56% of the variance in soil carbon content of which 35% was

276   explained by rock, 5% by water, 9% by plants and 19% by rock:plant interactions.

277   We next conducted a three-pool soil fractions to separate labile (free) POM, mineral and

278   aggregate components (SI Figure 2). The carbon content associated with the free POM

279   fraction decreased drastically over the course of the trial in all treatments from ~0.3% in the

280   baseline (red/blue line) to ~0.1% (Figure 3B). None of the treatments affected the free POM

281   loss. Rock addition significantly increased C associated with AggOM by 25% over the non-

282   amended control and by a massive 46% when only the non-planted treatments are considered

283   (Figure 3C). Plants counteracted the effect of rock-amendment on AggOM (rock:plant effect;

284   $p = 0.0002$). The carbon content associated with the MAOM fraction increased by 22%

285   because of rock addition and by 32% when only the non-planted treatments are considered

286   (Figure 3D). Rock-amendment significantly increased the amount of soil recovered as

287   MAOM (SI Figure 6A) but decreased the concentration of carbon within the MAOM fraction

288   by 14% ($p = 0.0002$; SI Figure 6B).

289   High water treatment resulted in significantly lower soil carbon levels than low water

290   treatment ($p = 0.00148$; Figure 3A). Water treatment only affected the carbon content

291   associated with MAOM fraction (Figure 3D; $p = 0.002$). This loss of carbon was not

292   associated with a lower carbon content within the MAOM fraction (SI Figure 6B), but instead

293   with less soil recovered in this fraction (SI Figure 6A; water effect: $p = 0.0006$).

3.3 Two-pool soil carbon fractionation and soil aggregates on a subset of samples

296   Using a two-pool soil carbon fractionation technique that ensures full disaggregation (and

297   hence separation of the AggOM pool into MAOM and free plus occluded POM) on a sub-set

298   of samples (Figure 4A; schematic SI Figure 2), both planted and unplanted rock treatments

299   significantly increased the carbon content associated with the MAOM fraction by ~0.07%

300   compared to the no-rock treatment. Rock addition also increased the POM fraction that

301   includes both occluded and free POM (Figure 4A1; $p = 0.006$), but only the unplanted, rock-

302   amended treatment was different to the control ($p = 0.005$; Figure 4A1). The aqueous fraction

303 that is used to extract the soil, contained dissolved organic matter (DOM) in the range of

304 0.12-0.15% carbon per unit of soil (SI Figure 7). There was a statistically significant increase

305 in the DOM pool in the rock, non-planted treatment compared to the control treatment

306 (ANOVA: p = 0.049; Tukey: p = 0.046).

307 In the same subset of samples, we analysed soil aggregation within aggregate size classes of

308 <70 µm to >1000 µm (Figure 4B). There was a statistically significant increase in

309 microaggregates of size 70-200 µm from 14.1% in the control to 22.2% in the unplanted,

310 rock-amended (Tukey post-hoc test: p = 0.004). Plants reduced the percentage of

311 microaggregates to 14.2%, fully counteracting the increase in microaggregation induced by

312 rock addition (Figure 4B).

3.4 Soil DNA and microbial composition

314 The extractable soil DNA content was significantly higher in rock-amended treatments

315 compared to unamended treatments (SI Figure 8A). The DNA content decreased over the

316 course of the trial compared to the baseline indicating that soil DNA was lost. There was a

317 significant correlation between soil DNA and soil carbon content (SI Figure 8B).

318 The total number of continuous DNA fragments (reads) extracted and sequenced per sample

319 were between 4,000 to 50,000 with an average read length of 600-3,000 base pairs (SI Table

320 3), generating >1Gb of sequence. The abundant microbial high level taxonomic groups

321 detected via shotgun metagenomics and long-read sequencing did not change significantly as

322 a result of rock addition as shown via clustering (SI Figure 9B) and percentage composition

323 (SI Figure 10). We also did not detect specific changes due to basalt or plant effects on

324 individual microbial taxa (SI Table 4). Water treatment, however, significantly affected

325 clustering of the samples based on phylum, class and order level (phylum level clustering in

326   SI Figure 9A (PERMANOVA results in SI Table 5). There were also significant effects

327   within the microbial taxa due to water treatment at the class and order level (SI Table 4).

3.5 Associations of soil properties with SOM fractions and SOM

  transformations

330   There was a highly significant correlation between soil exchangeable Ca and Mg contents

331   and soil carbon content ($p = 2.4 \times 10^{-7}$ and $p = 2.4 \times 10^{-10}$; Figure 5A,D) and a significant

332   correlation with Fe content ($p = 0.029$; Figure 5G). Exchangeable Ca and Mg contents also

333   correlated highly significantly with both carbon in AggOM (Figure 5B and E) and MAOM

334   (Figure 5C and F). Exchangeable Fe only correlated highly significantly with carbon as

335   AggOM ($p = 0.005$; Figure 5H).

336   The schematic in Figure 6A shows the effects of rock and rock-plant interactions on soil

337   carbon of different stability compared to the soil-only baseline and is based on Figure 3B-D.

338   Low- and high-water treatments were pooled to focus on plant and rock effects. C associated

339   with POM was reduced in all treatments compared to the baseline. However, depending on

340   treatment, the carbon was either lost or converted into different soil carbon fractions (Figure

341   6A). In the no-rock treatments, free POM was lost without any conversion into AggOM or

342   MAOM (C content as AggOM and MAOM same as in the baseline). In the rock amended

343   treatment, some free POM was instead retained as MAOM and as AggOM. In the non-

344   planted, rock amended treatment 12% of POM was lost and 19% in the treatment with plant.

345   Hence, the rock-amended, non-planted control retained 23% of free POM lost in the control

346   sample in the form of more stable soil carbon fractions.

4 Discussion

4.1 Inorganic carbon sequestration

Previous rock weathering studies have found it is challenging to directly detect changes to soil inorganic carbon content and therefore, typically proxies are used to assess rock weathering and associated drawdown of atmospheric CO_2. Such proxies include Ca and Mg mass balance approaches based on both pore water or ammonium acetate extractable cations and changes in pH and EC compared to a non-amended control (Amann et al., 2020; Amann & Hartmann, 2022; Kelland et al., 2020; ten Berge et al., 2012). In this study, we found elevated levels of water-extractable and exchangeable Ca and Mg contents and pH and EC levels in soil 6 months after rock addition. However, water-extractable Ca and Mg did not indicate additional weathering of our mining residues since the levels peaked at the start of the incubation (fresh rock-soil mix) and this peak was not associated with any (bi)carbonate formation (product of Ca- and Mg-rich silicate reaction with carbonic acid). Our mining residues had pre-weathered and contained 19.1% amorphous material and 3.9% secondary minerals, which likely contained cations that were only sorbed to mineral surfaces and were released without reacting with carbonic acid. These readily available cations would be responsible for this initial Ca and Mg release. Pre-weathering eliminates the Ca and Mg mass balance approach as proxy for new carbon drawdown and may be unsuitable for mining residues, at least if water extraction or pore water values are used.

There is some evidence for rock weathering based on exchangeable Ca and Mg contents, which were higher at the end of the trial compared to the rock-soil baseline. However, there is also no (extra) inorganic carbon detected in soil at the end of the incubation, as previously reported (Kelland et al., 2020). Overall, we could not find evidence for inorganic carbon formation in our trial. Only around half of the rock was composed of basalt and the

371   percentage of the fast-weathering mineral olivine was only 2%, which expectantly did not

372   result in a strong weathering signal at an application rate of 50 t ha^{-1}. Given the large range of

373   weathering rates and associated carbon drawdown rates in the literature, it is clear that the

374   method for determining weathering rates needs refinement. Other indirect weathering effects,

375   as presented here for SOM, do show potential.

4.2 Rock addition increases organic carbon protection

377   POM in sandy soil has little protection from decomposition and subsequently 2/3 of the POM

378   in the baseline soil was lost after 6 months of incubation under growing conditions (Figure

379   6A). Rock dust addition decreased SOM losses by transformation of POM into more durable

380   soil carbon fractions, and the effects were linked to changes in soil chemistry. We failed to

381   detect substantial abundance or composition shifts in the microbiome as a result of rock

382   addition (SI Figure 9). Our microbiome assay using shotgun, long-read sequences via Oxford

383   Nanopore Technology is robust and can detect differences among treatments in

384   environmental samples (Hamner et al., 2019; Loit et al., 2019; Petersen et al., 2020). Our

385   study shows that water treatment did have an effect on microbial composition as expected.

386   The soil response to rock addition can, however, be explained by three main chemical

387   changes that fostered SOM protection.

388   First, our rock mining residues were clearly pre-weathered (Table 1), therefore, the rocks

389   provided secondary silicate minerals immediately after application that were able to sorb

390   DOM directly. The concentration of carbon within MAOM of these rock-amended soils were

391   lower than their no-rock counterparts, which indicates potential for further carbon sorption

392   and hence MAOM formation with continuing rock weathering.

393   Secondly, rock provided Ca and Mg that are key cations involved in polyvalent cation

394   bridging and associated MAOM formation, along with Fe and Al. Ca and Mg mostly operate

395   in soil at neutral pH and Fe and Al in acidic conditions (Rowley et al., 2018; Singh et al.,

396   2018). Our baseline soil pH was slightly acidic with a pH of 5.7 in water and 4.9 in 0.01 M

397    $CaCl_2$, which increased to 6.2 in water (data not shown) and 5.2 in 0.01 M $CaCl_2$ at the end of

398   the incubation across all treatment. At this pH range both groups of cations are similarly

399   important in cation bridging, yet given our correlation analysis (Figure 5), exchangeable Ca

400   and Mg seemed to play a more important role in MAOM formation in our case.

401   Third, the results from both fractionation assays showed that rock clearly increased SOM

402   occluded within microaggregates. This increase in microaggregates and associated AggOM

403   can be explained by the supply of available Ca and Mg by the rock (Figure 6B), which

404   facilitated the formation of soil aggregates and carbon protection (Baldock, 1989; Clough &

405   Skjemstad, 2000; Rowley et al., 2018; Totsche et al., 2018). Our strong correlation between

406   soil exchangeable Ca and SOM content (Figure 5A) has also been seen in a previous study

407   (Rowley et al., 2018). In our trial, rock addition protected an extra 17% (Figure 6) (or

408   ~0.15% C in absolute values (Figure 3)) of soil carbon within AggOM that was lost without

409   rock addition. This effect could play a significant role in protection of POM from

410   decomposition, in particular in soil with low degree of aggregation and soil exchangeable Ca

411   and Mg levels.

412   Overall, the soil carbon content was 32% higher after rock amendment or 0.2% per weight of

413   soil. At a soil bulk density of 1.2 g cm^{-3} and a soil depth of 0.2 m this corresponds to 4.8 t of

414   extra stable carbon stored per hectare. While these results so far are only valid for sandy soils

415   of similar chemistry and cannot be extrapolated to larger areas globally, it does clearly

416   demonstrate the potential of ground rock application for sequestering additional organic

417   carbon. Plants, however, partially counteracted this effect.

4.3 Plant counteraction of protection of carbon in aggregates due to micronutrient deficiency

420 In the absence of rock, plants increased the soil carbon content (Figure 3). However, under

421 the altered chemical conditions after rock-amendment, plants reduced the protection of SOM

422 in aggregates (Figure 6B). It was shown previously that plant root exudates can accelerate the

423 turnover of aggregates, i.e., induce aggregate formation but also destruction (He et al., 2020;

424 Ma et al., 2022; Wang et al., 2020). Plants altered the chemical changes induced by rock

425 addition on SOM content and exchangeable cation levels.

426 Plants, including wheat, can increase root exudation as a response to nutrient deficiency to

427 solubilise micronutrients, such as Mn, Zn or Fe, to increase their availability and uptake

428 (Awad et al., 1994; Cakmak & Marschner, 1988; Gherardi & Rengel, 2004; F. Li et al.,

429 2018). Zn deficiency in various plant species, for example, increased root exudation by a

430 factor of 2 on average (Cakmak & Marschner, 1988). Such exudates include oxalate,

431 tartarate, L-malate, lactate, citrate and succinate (Gherardi & Rengel, 2004). The dramatic

432 drop in exchangeable micronutrient levels in our study after rock addition, as also observed

433 for Mn in a previous study after basalt application (Anda et al., 2015), and subsequent lower

434 plant uptake suggests exudation to solubilise micronutrients and increase plant uptake (Figure

435 6B). Availability of Mn and Zn decreases exponentially in the pH range of our soils (5-6.5)

436 through an increase of adsorbed Mn and Zn to soil surfaces (Basta et al., 2005). Rock

437 addition increased the pH by ~0.2 units within this pH range explaining the drop in

438 micronutrient availability.

439 Root exudates, such as oxalic acid/oxalate, increase micronutrient availability and hence

440 plant uptake. However, they can also strip polyvalent cations from their metalorganic ligand

441 complexes that results in both loss of cations and carbon (Keiluweit et al., 2015; F. Li et al.,

442   2018; H. Li et al., 2021). Fe does play a particularly important role in the formation of

443   microaggregates (52-250 um) (Z. Lin et al., 2022; Xue et al., 2019) and hence loss of Fe in

444   addition to Ca and Mg can explain the loss in microaggregates and carbon in AggOM in our

445   study. With a loss of Ca, Mg and Fe as mediators between clay surfaces and soil organic

446   carbon and cementation agents, soil aggregation decreased and hence less soil organic carbon

447   was stabilised. This shows the complexity of the system and how soil chemistry changes can

448   alter the effect of plants on SOM content, which in this case resulted in loss of soil carbon

449   with rock addition. Addressing micronutrient deficiencies should avoid the effect plants had

450   on soil aggregation and associated carbon contained within aggregates. Future studies should

451   be designed to specifically investigate this hypothesis.

Conclusion

We found evidence that a blend of granite and basalt applied to a sandy soil weathered during a 6-month incubation, as demonstrated by soil exchangeable Ca and Mg that were elevated compared to the baseline values. However, this was not associated with the expected increase in soil inorganic carbon content. Instead, rock addition increased SOM stabilisation through the release of Ca and Mg and provision of secondary minerals. A growing wheat plant partially counteracted this affect likely due to the release of plant root exudates induced by reductions in micronutrient levels, Mn and Zn, after rock addition and its associated pH increase. Such exudates solubilised, and hence induced losses of Ca, Mg and Fe that are typically involved in aggregate stabilisation, which also induced losses of carbon formerly protected in aggregates. Still, the application of Ca- and Mg-rich silicates can be a valuable tool to stabilise SOM, particularly in sandy soil and when micronutrient deficiencies are addressed. This could substantially improve the carbon sequestration potential of ground rock application on agricultural land. Higher soil organic carbon levels can have further soil and plant benefits, such as increasing nutrient and water retention. These findings could boost the economic and environmental attractiveness of enhanced rock weathering as a global method for carbon dioxide removal.

Acknowledgement

References

477   Abramoff, R., Xu, X., Hartman, M., O'Brien, S., Feng, W., Davidson, E., Finzi, A.,

478   Moorhead, D., Schimel, J., Torn, M., & Mayes, M. A. (2018). The Millennial model: in

479   search of measurable pools and transformations for modeling soil carbon in the new

480   century. *Biogeochemistry*, *137*(1–2), 51–71. https://doi.org/10.1007/s10533-017-0409-7

482   Alvarez, R. (2005). A review of nitrogen fertilizer and conservation tillage effects on soil

483   organic carbon storage. *Soil Use and Management*, *21*(1), 38–52.

484   https://doi.org/10.1079/sum2005291

485   Amann, T., & Hartmann, J. (2022). Carbon Accounting for Enhanced Weathering. *Frontiers*

486   *in Climate*, *4*. https://doi.org/10.3389/fclim.2022.849948

487   Amann, T., Hartmann, J., Struyf, E., De Oliveira Garcia, W., Fischer, E. K., Janssens, I.,

488   Meire, P., & Schoelynck, J. (2020). Enhanced Weathering and related element fluxes -

489   A cropland mesocosm approach. *Biogeosciences*, *17*(1), 103–119.

490   https://doi.org/10.5194/bg-17-103-2020

491   Amezketa, E. (1999). Soil aggregate stability: A review. *Journal of Sustainable Agriculture*,

492   *14*, 83–151. https://doi.org/10.1300/J064v14n02

493   Anda, M., Shamshuddin, J., & Fauziah, C. I. (2015). Improving chemical properties of a

494   highly weathered soil using finely ground basalt rocks. *Catena*, *124*, 147–161.

495   https://doi.org/10.1016/j.catena.2014.09.012

496   Awad, E., Romheld, V., & Marschner, H. (1994). Effect of root exudates on mobilization in

497   the rhizosphere and uptake of iron by wheat plants. In *Plant and Soil* (Vol. 165). Kluwer

498   Academic Publ&hers.

499   Baldock, J. (1989). *Influence of calcium on the decomposition of organic materials in soils*

500   [PhD Thesis]. The University of Adelaide.

501   Basta, N. T., Ryan, J. a, & Chaney, R. L. (2005). Trace element chemistry in residual-treated

502   soil: key concepts and metal bioavailability. *Journal of Environmental Quality*, *34*(1),

503   49–63. http://www.ncbi.nlm.nih.gov/pubmed/15647534

504   Beerling, D. J., Leake, J. R., Long, S. P., Scholes, J. D., Ton, J., Nelson, P. N., Bird, M.,

505   Kantzas, E., Taylor, L. L., Sarkar, B., Kelland, M., Delucia, E., Kantola, I., Müller, C.,

506   Rau, G. H., & Hansen, J. (2018). Climate, Food and Soil Security. *Nature Plants*,

507   *4*(March), 138–147. https://doi.org/10.1038/s41477-018-0108-y

508   Bormann, B. T., Wang, D., Bormann, F. H., Benoit, G., April, R., & Snyder, M. C. (1998).

509   Rapid, plant-induced weathering in an aggrading experimental ecosystem.

510   *Biogeochemistry*, *43*(2), 129–155. https://doi.org/10.1023/A:1006065620344

511   Brady, P. V., Dorn, R. I., Brazel, A. J., Clark, J., Moore, R. B., & Glidewell, T. (1999). Direct

512   measurement of the combined effects of lichen, rainfall, and temperature onsilicate

513   weathering. *Geochimica et Cosmochimica Acta*, *63*(19–20), 3293–3300.

514   https://doi.org/10.1016/S0016-7037(99)00251-3

515   Buss, W., Sharma, R., Ferguson, S., & Borevitz, J. (2021). Soil organic carbon fractionation

516   and metagenomics pipeline to link carbon content and stability with microbial

517   composition – First results investigating fungal endophytes. *BioRxiv, PREPRINT*.

518   Buss, W., Yeates, K., Rohling, E. J., & Borevitz, J. (2021). Enhancing natural cycles in agro-

519   ecosystems to boost plant carbon capture and soil storage. *Oxford Open Climate*

520   *Change*, *1*(1), kgab006. https://doi.org//10.1093/oxfclm/kgab006

521   Cakmak, I., & Marschner, H. (1988). Increase in Membrane Permeability and Exudation in

522   Roots of Zinc Deficient Plants. *Journal of Plant Physiology*, *132*(3), 356–361.

523   https://doi.org/10.1016/S0176-1617(88)80120-2

524   Clough, A., & Skjemstad, J. O. (2000). Physical and chemical protection of soil organic

525   carbon in three agricultural soils with different contents of calcium carbonate. *Australian*

526   *Journal of Soil Research*, *38*(5), 1005–1016. https://doi.org/10.1071/SR99102

527   Cochran, M. F., & Berner, R. A. (1996). Promotion of chemical weathering by higher plants:

528   field observations on Hawaiian basalts. *Chemical Geology*, *132*, 71–77.

529   Cotrufo, M. F., Ranalli, M. G., Haddix, M. L., Six, J., & Lugato, E. (2019). Soil carbon

530   storage informed by particulate and mineral-associated organic matter. *Nature*

531   *Geoscience*, *12*(12), 989–994. https://doi.org/10.1038/s41561-019-0484-6

532   De Coster, W., Hert, S. D., Schultz, D. T., Cruts, M., & Broeckhoven, C. Van. (2018).

533   NanoPack: visualizing and processing long-read sequencing data. *Bioinformatics*,

534   *34*(March), 2666–2669. https://doi.org/10.1093/bioinformatics/bty149

535   Fuss, S., Lamb, W. F., Callaghan, M. W., Hilaire, J., Creutzig, F., Amann, T., Beringer, T.,

536   De Oliveira Garcia, W., Hartmann, J., Khanna, T., Luderer, G., Nemet, G. F., Rogelj, J.,

537   Smith, P., Vicente, J. V., Wilcox, J., Del Mar Zamora Dominguez, M., & Minx, J. C.

538   (2018). Negative emissions - Part 2: Costs, potentials and side effects. *Environmental*

539   *Research Letters*, *13*(6). https://doi.org/10.1088/1748-9326/aabf9f

540   Gherardi, M. J., & Rengel, Z. (2004). The effect of manganese supply on exudation of

541   carboxylates by roots of lucerne (Medicago sativa). In *Plant and Soil* (Vol. 260).

542   Hamner, S., Brown, B. L., Hasan, N. A., Franklin, M. J., Doyle, J., Eggers, M. J., Colwell, R.

543   R., & Ford, T. E. (2019). Metagenomic profiling of microbial pathogens in the little

544   bighorn river, Montana. *International Journal of Environmental Research and Public*

545   *Health*, *16*(7). https://doi.org/10.3390/ijerph16071097

546 Haque, F., Santos, R. M., & Chiang, Y. W. (2020). Optimizing Inorganic Carbon

547   Sequestration and Crop Yield With Wollastonite Soil Amendment in a Microplot Study.

548   *Frontiers in Plant Science*, *11*(July), 1–12. https://doi.org/10.3389/fpls.2020.01012

549 Haque, F., Santos, R. M., Dutta, A., Thimmanagari, M., & Chiang, Y. W. (2019). Co-

550   Benefits of Wollastonite Weathering in Agriculture: CO2 Sequestration and Promoted

551   Plant Growth [Research-article]. *ACS Omega*, *4*(1), 1425–1433.

552   https://doi.org/10.1021/acsomega.8b02477

553 Hartmann, J., West, A. J., Renforth, P., Köhler, P., De La Rocha, C. L., Wolf-Gladrow, D.

554   A., Dürr, H. H., & Scheffran, J. (2013). Enhanced chemical weathering as a

555   geoengineering strategy to reduce atmospheric carbon dioxide, supply nutrients, and

556   mitigate ocean acidification. *Reviews of Geophysics*, *51*(2), 113–149.

557   https://doi.org/10.1002/rog.20004

558 He, Y., Cheng, W., Zhou, L., Shao, J., Liu, H., Zhou, H., Zhu, K., & Zhou, X. (2020). Soil

559   DOC release and aggregate disruption mediate rhizosphere priming effect on soil C

560   decomposition. *Soil Biology and Biochemistry*, *144*.

561   https://doi.org/10.1016/j.soilbio.2020.107787

562 Hemingway, J. D., Rothman, D. H., Grant, K. E., Rosengard, S. Z., Eglinton, T. I., Derry, L.

563   A., & Galy, V. v. (2019). Mineral protection regulates long-term global preservation of

564   natural organic carbon. *Nature*, *570*(7760), 228–231. https://doi.org/10.1038/s41586-

565   019-1280-6

566   Hinsinger, P., Fernandes Barros, O. N., Benedetti, M. F., Noack, Y., & Callot, G. (2001).

567   Plant-induced weathering of a basaltic rock: Experimental evidence. *Geochimica et*

568   *Cosmochimica Acta*, *65*(1), 137–152. https://doi.org/10.1016/S0016-7037(00)00524-X

569   Holdren, G. R., & Speyer, P. M. (1985). Reaction rate-surface area relationships during the

570   early stages of weathering. I. Initial observations. *Geochimica et Cosmochimica Acta*,

571   *51*(9), 2311–2318. https://doi.org/10.1016/0016-7037(87)90284-5

572   IPCC. (2022). *Climate Change 2022: Mitigation of Climate Change. Contribution of*

573   *Working Group III to the Sixth Assessment Report of the Intergovernmental Panel on*

574   *Climate Change* (P. Shukla, J. Skea, P. Shukla, A. Al Khourdajie, R. van Diemen, D.

575   McCollum, M. Pathak, S. Some, P. Vyas, R. Fradera, M. Belcacemi, A. Hasuja, G.

576   Lisboa, S. Luz, & J. Malley, Eds.). Cambridge University Press.

577   https://doi.org/10.1017/9781009157926

578   Keiluweit, M., Bougoure, J. J., Nico, P. S., Pett-ridge, J., Weber, P. K., & Kleber, M. (2015).

579   Mineral protection of soil carbon counteracted by root exudates. *Nature Climate*

580   *Change*, *5*(June), 588–595. https://doi.org/10.1038/NCLIMATE2580

581   Kelland, M. E., Wade, P. W., Lewis, A. L., Taylor, L. L., Sarkar, B., Andrews, M. G.,

582   Lomas, M. R., Cotton, T. E. A., Kemp, S. J., James, R. H., Pearce, C. R., Hartley, S. E.,

583   Hodson, M. E., Leake, J. R., Banwart, S. A., & Beerling, D. J. (2020). Increased yield

584   and CO2 sequestration potential with the C4 cereal Sorghum bicolor cultivated in

585   basaltic rock dust-amended agricultural soil. *Global Change Biology*, *March*, 1–19.

586   https://doi.org/10.1111/gcb.15089

587   Kleber, M., Eusterhues, K., Keiluweit, M., Mikutta, C., Mikutta, R., & Nico, P. S. (2015).

588   Mineral-Organic Associations: Formation, Properties, and Relevance in Soil

589   Environments. *Advances in Agronomy*, *130*, 1–140.

590   https://doi.org/10.1016/bs.agron.2014.10.005

591   Kuzyakov, Y. (2010). Priming effects: Interactions between living and dead organic matter.

592   *Soil Biology and Biochemistry*, *42*(9), 1363–1371.

593   https://doi.org/10.1016/j.soilbio.2010.04.003

594   Lavallee, J. M., Soong, J. L., & Cotrufo, M. F. (2020). Conceptualizing soil organic matter

595   into particulate and mineral-associated forms to address global change in the 21st

596   century. *Global Change Biology*, *26*(1), 261–273. https://doi.org/10.1111/gcb.14859

597   Li, F., Koopal, L., & Tan, W. (2018). Roles of different types of oxalate surface complexes in

598   dissolution process of ferrihydrite aggregates. *Scientific Reports*, *8*(1).

599   https://doi.org/10.1038/s41598-018-20401-5

600   Li, G., Hartmann, J., Derry, L. A., West, A. J., You, C., Long, X., Zhan, T., Li, L., Li, G.,

601   Qiu, W., Li, T., Liu, L., Chen, Y., Ji, J., Zhao, L., & Chen, J. (2016). Temperature

602   dependence of basalt weathering. *Earth and Planetary Science Letters*, *443*, 59–69.

603   https://doi.org/10.1016/j.epsl.2016.03.015

604   Li, H., Bolscher, T., Winnick, M., Tfaily, M. M., Cardon, Z. G., & Keiluweit, M. (2021).

605   Simple plant and microbial exudates destabilize mineral-Associated organic matter via

606   multiple pathways. *Environmental Science and Technology*, *55*(5), 3389–3398.

607   https://doi.org/10.1021/acs.est.0c04592

608   Lin, H., & Peddada, S. Das. (2020). Analysis of compositions of microbiomes with bias

609   correction. *Nature Communications*, *11*(1). https://doi.org/10.1038/s41467-020-17041-7

610   Lin, Z., Huang, Z. gang, Liao, D. lan, Huang, W. xia, Huang, J., & Deng, Y. song. (2022).

611   Effects of soil organic matter components and iron aluminum oxides on aggregate

612 stability during vegetation succession in granite red soil eroded areas. *Journal of*

613 *Mountain Science*, *19*(9), 2634–2650. https://doi.org/10.1007/s11629-021-7185-5

614 Loit, K., Adamson, K., Bahram, M., Puusepp, R., Anslan, S., Kiiker, R., Drenkhan, R., &

615 Tedersoo, L. (2019). Relative Performance of MinION (Oxford Nanopore Technologies)

616 versus Sequel (Pacific Biosciences) Third-Generation Sequencing Instruments in

617 Identification of Agricultural and Forest Fungal Pathogens. *Applied and Environmental*

618 *Microbiology*, *85*(21), 1–20. https://doi.org/10.1128/AEM

619 Luo, Z., Feng, W., Luo, Y., Baldock, J., & Wang, E. (2017). Soil organic carbon dynamics

620 jointly controlled by climate, carbon inputs, soil properties and soil carbon fractions.

621 *Global Change Biology*, *23*(10), 4430–4439. https://doi.org/10.1111/gcb.13767

622 Ma, W., Tang, S., Dengzeng, Z., Zhang, D., Zhang, T., & Ma, X. (2022). Root exudates

623 contribute to belowground ecosystem hotspots: A review. In *Frontiers in Microbiology*

624 (Vol. 13). Frontiers Media S.A. https://doi.org/10.3389/fmicb.2022.937940

625 Petersen, L. M., Martin, I. W., Moschetti, W. E., Kershaw, C. M., & Tsongalis, G. J. (2020).

626 Third-Generation Sequencing in the Clinical Laboratory: Exploring the Advantages and

627 Challenges of Nanopore Sequencing. *Journal of Clinical Microbiology*, *58*(1), 1–10.

628 https://journals.asm.org/journal/jcm

629 Poeplau, C., Don, A., Six, J., Kaiser, M., Benbi, D., Chenu, C., Cotrufo, M. F., Derrien, D.,

630 Gioacchini, P., Grand, S., Gregorich, E., Griepentrog, M., Gunina, A., Haddix, M.,

631 Kuzyakov, Y., Kühnel, A., Macdonald, L. M., Soong, J., Trigalet, S., … Nieder, R.

632 (2018). Isolating organic carbon fractions with varying turnover rates in temperate

633 agricultural soils – A comprehensive method comparison. *Soil Biology and*

634 *Biochemistry*, *125*(June 2017), 10–26. https://doi.org/10.1016/j.soilbio.2018.06.025

635   Poeplau, C., Sigurdsson, P., & Sigurdsson, B. D. (2020). Depletion of soil carbon and

636   aggregation after strong warming of a subarctic Andosol under forest and grassland

637   cover. *SOIL*, *6*(1), 115–129. https://doi.org/10.5194/soil-6-115-2020

638   Renforth, P. (2012). The potential of enhanced weathering in the UK. *International Journal*

639   *of Greenhouse Gas Control*, *10*, 229–243. https://doi.org/10.1016/j.ijggc.2012.06.011

640   Rowley, M. C., Grand, S., & Verrecchia, É. P. (2018). Calcium-mediated stabilisation of soil

641   organic carbon. *Biogeochemistry*, *137*(1–2), 27–49. https://doi.org/10.1007/s10533-017-

642   0410-1

643   Sayers, E. W., Beck, J., Bolton, E. E., Bourexis, D., Brister, J. R., Canese, K., Comeau, D. C.,

644   Funk, K., Kim, S., Klimke, W., Marchler-Bauer, A., Landrum, M., Lathrop, S., Lu, Z.,

645   Madden, T. L., O'Leary, N., Phan, L., Rangwala, S. H., Schneider, V. A., … Sherry, S.

646   T. (2021). Database resources of the National Center for Biotechnology Information.

647   *Nucleic Acids Research*, *49*(October 2020), 10–17. https://doi.org/10.1093/nar/gkaa892

648   Singh, M., Sarkar, B., Sarkar, S., Churchman, J., Bolan, N., Mandal, S., Menon, M.,

649   Purakayastha, T. J., & Beerling, D. J. (2018). Stabilization of Soil Organic Carbon as

650   Influenced by Clay Mineralogy. *Advances in Agronomy*, *148*, 33–84.

651   https://doi.org/10.1016/bs.agron.2017.11.001

652   Taylor, J. C. (1991). Computer Programs for Standardless Quantitative Analysis of Minerals

653   Using the Full Powder Diffraction Profile. *Powder Diffraction*, *6*(1), 2–9.

654   https://doi.org/10.1017/S0885715600016778

655   ten Berge, H. F. M., van der Meer, H. G., Steenhuizen, J. W., Goedhart, P. W., Knops, P., &

656   Verhagen, J. (2012). Olivine weathering in soil, and its effects on growth and nutrient

657   uptake in ryegrass (Lolium perenne L.): A pot experiment. *PLoS ONE*, *7*(8).

658   https://doi.org/10.1371/journal.pone.0042098

659   Totsche, K. U., Amelung, W., Gerzabek, M. H., Guggenberger, G., Klumpp, E., Knief, C.,

660   Lehndorff, E., Mikutta, R., Peth, S., Prechtel, A., Ray, N., & Kögel-Knabner, I. (2018).

661   Microaggregates in soils. In *Journal of Plant Nutrition and Soil Science* (Vol. 181, Issue

662   1, pp. 104–136). Wiley-VCH Verlag. https://doi.org/10.1002/jpln.201600451

663   Wang, X., Yin, L., Dijkstra, F. A., Lu, J., Wang, P., & Cheng, W. (2020). Rhizosphere

664   priming is tightly associated with root-driven aggregate turnover. *Soil Biology and*

665   *Biochemistry*, *149*. https://doi.org/10.1016/j.soilbio.2020.107964

666   White, A. F., & Blum, A. E. (1995). Effects of climate on chemical weathering in watersheds.

667   *Water-Rock Interaction. Proc. Symposium, Vladivostok, 1995*, *59*(9), 57–60.

668   Wiesmeier, M., Urbanski, L., Hobley, E., Lang, B., von Lützow, M., Marin-Spiotta, E., van

669   Wesemael, B., Rabot, E., Ließ, M., Garcia-Franco, N., Wollschläger, U., Vogel, H. J., &

670   Kögel-Knabner, I. (2019). Soil organic carbon storage as a key function of soils - A

671   review of drivers and indicators at various scales. *Geoderma*, *333*(July 2018), 149–162.

672   https://doi.org/10.1016/j.geoderma.2018.07.026

673   Xue, B., Huang, L., Huang, Y., Yin, Z., Li, X., & Lu, J. (2019). Effects of organic carbon and

674   iron oxides on soil aggregate stability under different tillage systems in a rice–rape

675   cropping system. *Catena*, *177*, 1–12. https://doi.org/10.1016/j.catena.2019.01.035

676

Table 1: Characterisation of rock sample.

Mineralogy	(%)
Amorphous	19.1
Quartz	16.3
Plagioclase	34.4
K-feldspar	5.7
Clinopyroxene	10.4
Olivine	2
Nepheline	1.2
Analcime	1.3
Apatite	1.3
Kaolinite	0.2
Mica	4.4
2:1 Clay	3.7
* Chlorite, Vermiculite or Smectite	

Elemental content	(%)
Al_2O_3	13.4
BaO	0.04
CaO	4.67
Cr_2O_3	0.05
Fe_2O_3	8.12
K_2O	2.65
MgO	4.13
MnO	0.10
Na_2O	3.24
P_2O_5	0.42
SiO_2	60.9
SrO	0.05
TiO_2	1.41

Particle size	(%)
<90	96.5
<70	89.3
<50	80.1
<10	29.6

Loss on ignition	0.68
pH (in water)	9.2
C content (%)	0.075

A Soil inorganic carbon content (%)

B Soil pH in 0.01 M CaCl$_2$ (-)
rock: p = 0.000006

C Soil EC (uS cm^{-1})
rock: p = 1.2 x 10^{-9} plant: p = 0.0009
water: p = 8 x 10^{-5}

D Soil water-extractable Ca (mg kg^{-1})
rock:plant: p = 0.00535
rock: p = 1.6 x 10^{-9} plant: p = 9 x 10^{-11}

E Soil water-extractable Mg (mg kg^{-1})
rock: 1.6 x 10^{-8} plant: p = 1 x 10^{-7}
water: p = 0.0231

F Soil water-extractable Si (mg kg^{-1})

G Soil exchangeable Ca (mg kg^{-1})
rock:plant: p = 9.7 x 10^{-6}
rock: p = <2 x 10^{-16} plant: p = 0.001
plant:water: p = 0.00096   water: p = 0.018

H Soil exchangeable Mg (mg kg^{-1})
rock: <2 x 10^{-16} rock:plant: p = 1.28 x 10^{-11}

I Soil exchangeable Si (mg kg^{-1})
rock: <2 x 10^{-16} water: p = 0.0029

low high low high
no plant   plant
no rock
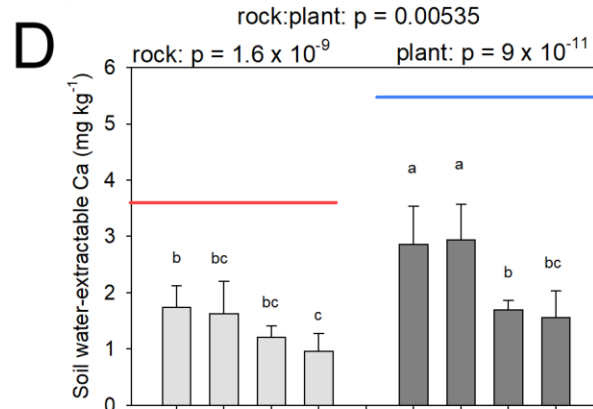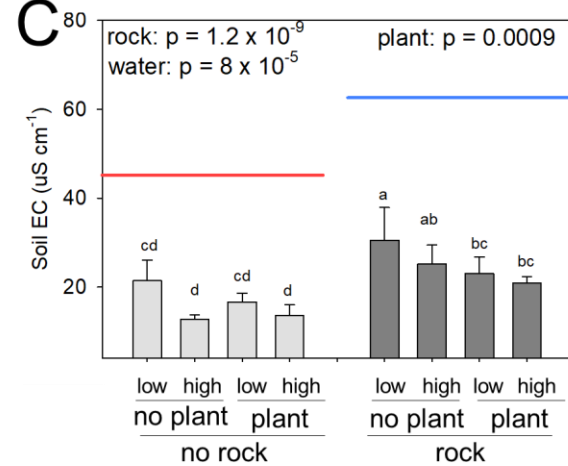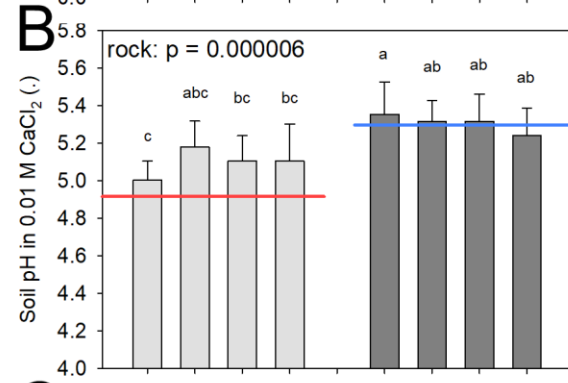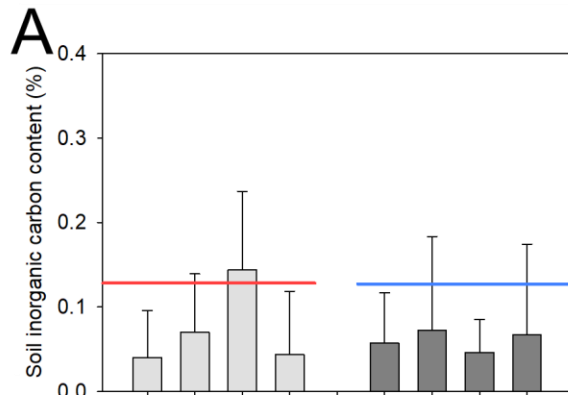
low high low high
no plant   plant
rock

Figure 1: Soil indicators for weathering of Ca- and Mg-rich silicate rocks at the end of 6-month incubation. (A) Inorganic carbon content, (B) pH, (C) EC, and (D) water-extractable Ca, (E) Mg and (F) Si contents and ammonium acetate-extractable (exchangeable) (G) Ca, (H) Mg and (I) Si contents. Soil was analysed at the end of a 6-month incubation study using a full factorial design with high/low water, unplanted/planted soil and soil only/rock addition. Red and blue lines indicate baseline values from the soil at the start of the trial without and with rock addition (~4%), respectively. Main effects determined using one-way ANOVAs (results shown at the top of each figure). Different letters indicate significant differences among the treatments determined via Tukey post-hoc test.
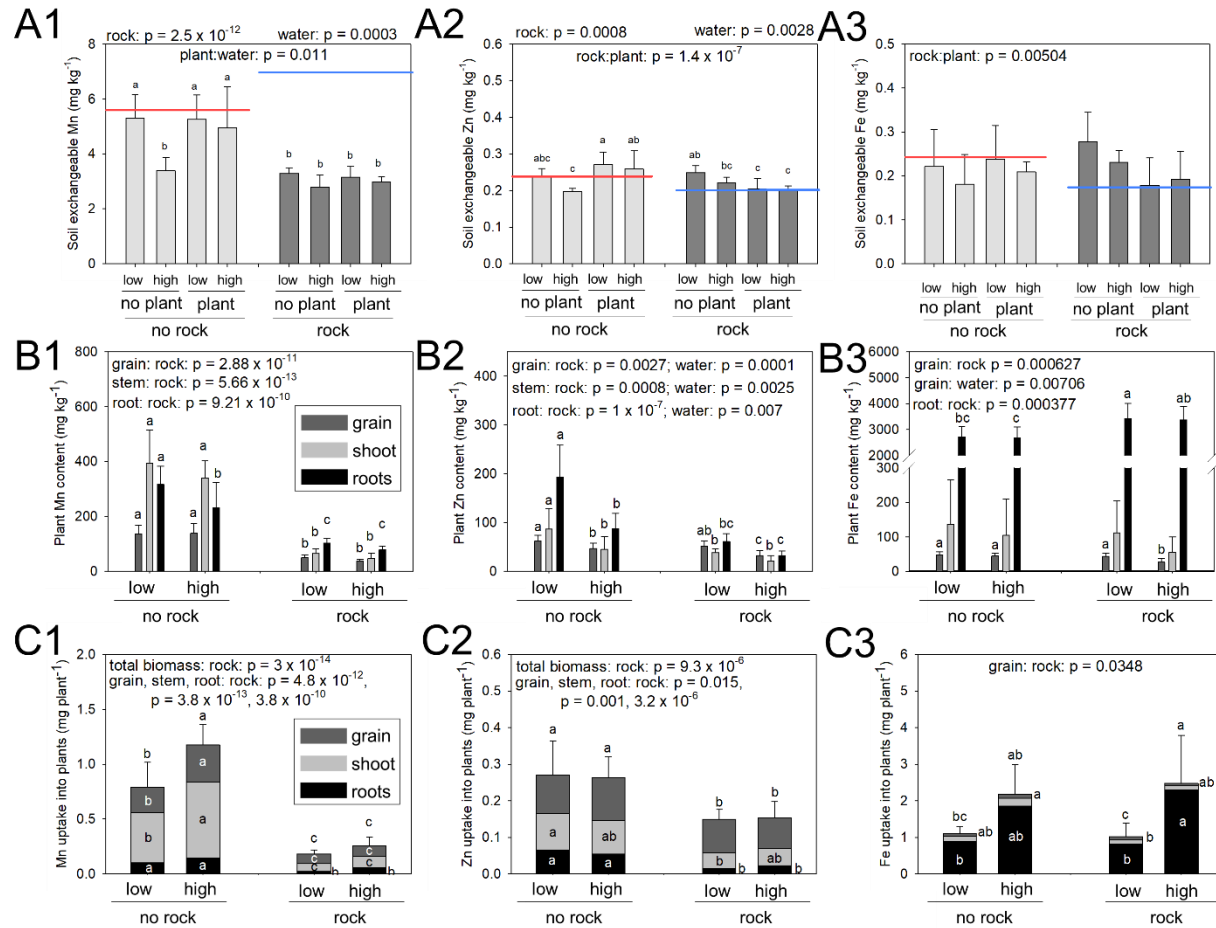
Figure 2: Micronutrients Mn (1), Zn (2) and (3) Fe in plant and soil at the end of 6-month incubation. (A) Ammonium acetate exchangeable contents for soils in all 8 treatments, and (B) plant tissue contents of grain, shoots and roots and (C) total plant uptake in grain, shoot and roots for the planted treatments. Red and blue lines indicate baseline values from the soil at the start of the trial without and with rock addition (~4%),

respectively. Main effects determined using one-way ANOVAs (results shown at the top of each figure). Different letters indicate significant differences among the treatments determined via Tukey post-hoc test.
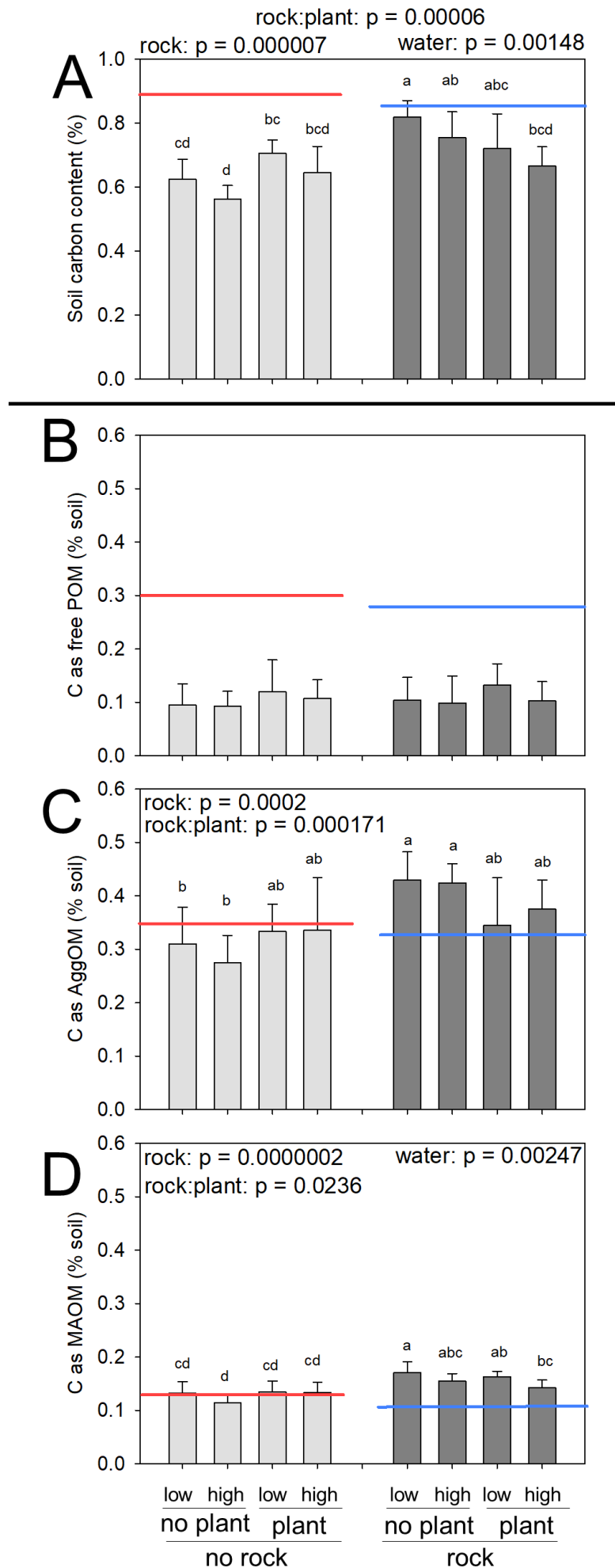
Figure 3: (A) Total soil carbon content and (B-D) three-pool soil carbon fractionation data at the end of 6-month incubation. (B-D) show carbon associated with (B) particulate organic matter (POM), (C) aggregate organic matter (AggOM) and (D) mineral-associated organic matter (MAOM). A full factorial design of high/low water, unplanted/planted soil and soil only/rock addition was used. Red and blue lines indicate baseline values from the soil at the start of the trial without and with rock addition (~4%), respectively. Main effects determined using one-way ANOVAs (results shown at the top of each figure). Different letters indicate significant differences among the treatments determined via Tukey post-hoc test.
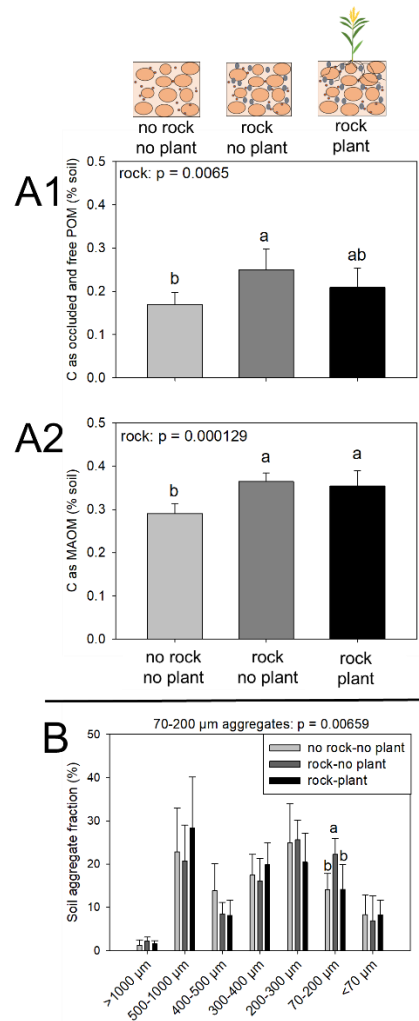
Figure 4: (A) Soil carbon occlusion determined via 2-pool soil fractionation and (B) soil aggregates in a subset of samples. Treatments: no rock without plant (control-control-low), rock with and without plants (all low water treatments). (A) Soil carbon fractionation using hexameta-phosphate extraction for full soil disaggregation at the end of a 6-months incubation. Carbon associated with the (A1) free and occluded POM fraction and (A2) MAOM fraction. Main effects determined using one-way ANOVAs (results shown at the top of each figure). Different letters indicate significant differences among the treatments determined via Tukey post-hoc test. (B) Soil aggregate classes. For statistical analysis (ANOVA, followed by Tukey's post-hoc test), data were centred log ratio transformed.
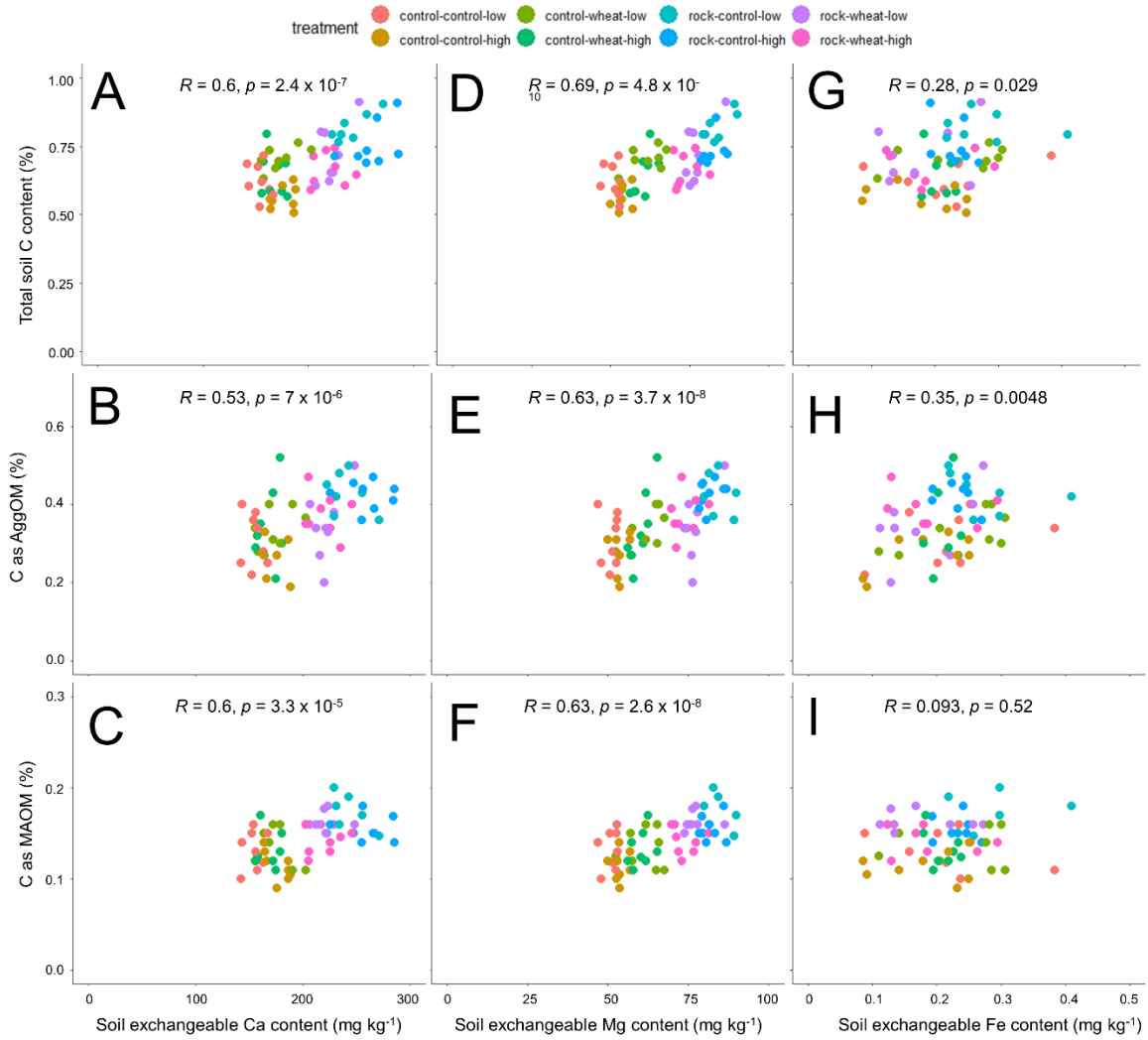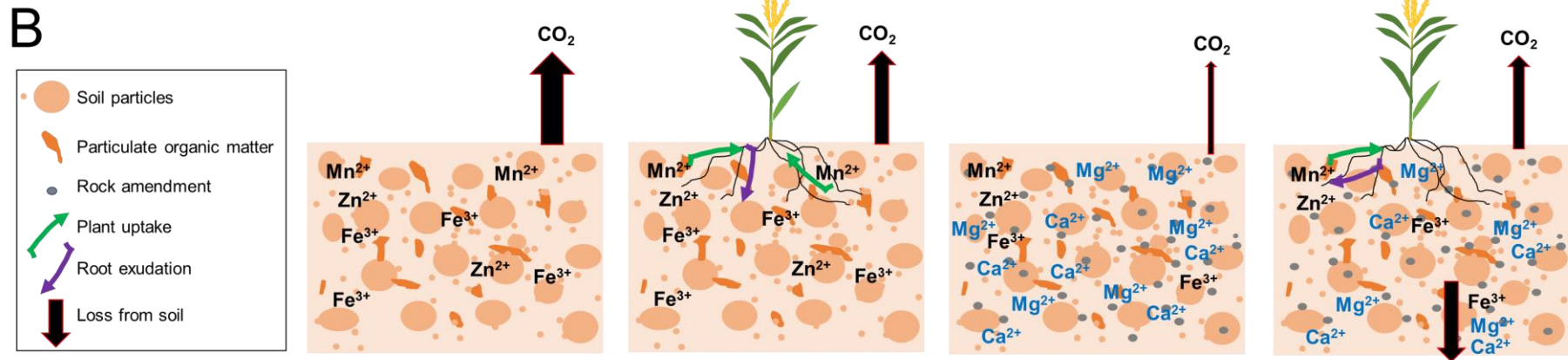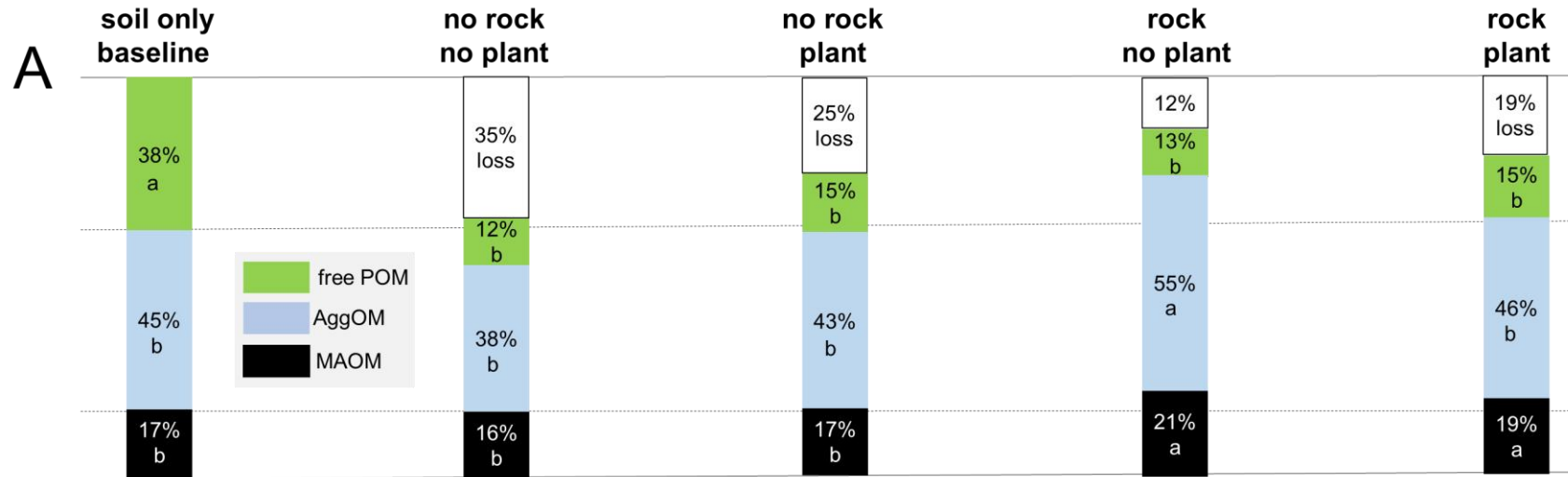
Figure 5: Relationship of soil exchangeable (A-C) Ca, (D-F) Mg and (G-H) Fe contents with (A, D, G) total soil C content, (B, E, H) C associated with AggOM and (C, F, I) C associated with MAOM at the end of 6-months incubation. Treatment labels are control/rock - control/wheat - low/high water. Pearson correlation coefficient and p-value shown, respectively.

A

soil only baseline	no rock no plant	no rock plant	rock no plant	rock plant

soil only baseline
- 38% a (free POM)
- 45% b (AggOM)
- 17% b (MAOM)

no rock no plant
- 35% loss
- 12% b (free POM)
- 38% b (AggOM)
- 16% b (MAOM)

no rock plant
- 25% loss
- 15% b (free POM)
- 43% b (AggOM)
- 17% b (MAOM)

rock no plant
- 12% (loss)
- 13% b (free POM)
- 55% a (AggOM)
- 21% a (MAOM)

rock plant
- 19% loss
- 15% b (free POM)
- 46% b (AggOM)
- 19% a (MAOM)

Legend:
- free POM (green)
- AggOM (light blue)
- MAOM (black)

B

Legend:
- Soil particles
- Particulate organic matter
- Rock amendment
- Plant uptake (green arrow)
- Root exudation (purple arrow)
- Loss from soil (black arrow)

CO_2

Panel ions shown: Mn^{2+}, Zn^{2+}, Fe^{3+}, Mg^{2+}, Ca^{2+}

	soil only baseline	no rock no plant	no rock plant	rock no plant	rock plant
Soil micronutrient availability / plant uptake (Zn, Mn and Fe)		High / NA	High / high	Low / NA	Low / low
Soil Ca and Mg availability		Low	Low-medium	High	High-medium
Soil POM content		Low	Low	Low	Low
Soil AggOM content		Unchanged	Unchanged	High	Unchanged
Soil MAOM content		Unchanged	Unchanged	High	High
Hypothesis mechanisms behind SOM response		Limited protection of POM through aggregates and mineral surfaces	Plants increase carbon through exudation but soil provides limited POM protection	Mg and Ca increase POM stability through carbon protection in aggregates and sorption to mineral surfaces	Low Mn/Zn/Fe availability leads to plant exudation that solubilises and removes Ca, Mg and Fe from soil, which reduces POM protection in aggregates

Figure 6: Summary of soil (carbon) responses to rock and plant additions relative to the soil baseline. (A) Conversion of SOM fractions in the baseline scenario (soil before trial) into other soil carbon fractions based on data in Figure 3 (low- and high-water treatments pooled together, n = 16). Letters show significant differences among the treatments. (B) Schematic summary of the key results.